Astronomy & Astrophysics manuscript no. output

September 10, 2026

High-Energy Solar Particle Hits Detected with the Extreme Ultraviolet Imager onboard Solar Orbiter

A Report on Particle Event Statistics and Energy Characterization

K. Barczynski[1,2]⋆ and N. P. Janitzek[3]⋆⋆

[1] Physical Meteorological Observatory Davos (PMOD), Dorfstrasse 33, 7260 Davos Dorf, Switzerland
[2] Institute for Particle Physics and Astrophysics, Swiss Federal Institute of Technology (ETH) Zürich, Wolfgang-Pauli-Strasse 27, 8093 Zürich, Switzerland
[3] European Space Agency (ESA), European Space Astronomy Centre (ESAC), Camino Bajo del Castillo, s/n, 28692 Villanueva de la Cañada, Madrid, Spain

Received September 30, 20XX

ABSTRACT

Context. This is a technical note on the detection of Solar Energetic Particles (SEPs) using the Extreme Ultraviolet Imager (EUI) onboard Solar Orbiter.

Aims. Our aim is to present an automated method to detect Solar Energetic Particle (SEP) which interact with EUI/FSI detector. Characterize their occurrence and compare them with EPD particle measurements.

Methods. EUI/FSI images are divided into 5×5-pixel blocks and analyzed for significant intensity outliers. SEP detections are identified using an intensity mean and standard deviation related threshold based on comparison with EPD observations.

Results. SEP events produce a clear increase in the number of particle hits detected by EUI/FSI. We create a software for SEP event detection, and the using this softare, we created a catalogue of SEP events affecting EUI/FSI

Key words. Sun – particles – test

Use \titlerunning to supply a shorter title and/or \authorrunning to supply a shorter list of authors.

1. Introduction

The Sun generates a quasi-continuous flow of charged particles known as the solar wind. These particles are protons, electrons, and heavy ions. In addition to this nearly steady outflow, solar events occur spontaneously and can lead to the emission of solar energetic particles (SEPs). These events, such as solar flares, which produce intense bursts of electromagnetic radiation, and coronal mass ejections (CMEs), which involve the large-scale ejection of plasma from the solar atmosphere, can accelerate particles to speeds much above the solar wind speed range and therefore produce fast, highly energetic particle populations.

High-energy particles in space can have a significant impact on modern technology, particularly spacecraft instrumentation and electronics. They can produce single-event effects, such as corrupting computer memory, causing anomalies in instrument operation, and, in extreme cases, permanently damaging electronic components. In imaging space-based instruments, energetic particle events can significantly affect a detector and can generate strong and localized signals on the detector. This implies an increase in the apparent noise level which can even strongly disturb the actual photon signal.

Often, these disturbing effects of energetic particles in astronomical imaging detectors are referred to as cosmic ray hits (CRHs) and algorithms have been developed to detect, quantify and filter out these signals. Yet, to fully understand the effect of particle radiation on such CMOS and CCD sensors, it is also important to take into account the origin of the radiation. In particular, for space missions in the inner heliosphere the high-energy ion radiation that originates from the Sun plays an important role. This is due to the fact, that despite being typically less energetic than e.g. Galactic Cosmic Radiation (GCR), these SEP ions reach much higher intensities in strong solar events up to the energy range of a few hundred MeV/nuc. At these energies, the ions can already penetrate substantial payload shielding and affect the imaging detectors and electronics in the above described way. Therefore, understanding the impact of the SEPs - as part of the overall energetic particle hits - is essential for protecting space instrumentation and assessing the quality and reliability of observations obtained by spaceborne imaging instruments.

Most solar missions observe the Sun from an Earth-bound orbit. In contrast, Solar Orbiter is the first mission to combine simultaneous observations from remote-sensing and in-situ instruments from a heliocentric orbit that reaches distances as close as 0.29. These close distances to the Sun do not only imply a harsh particle radiation environment but also the need of a heatshield at the boreside of the spacecraft to keep the payload operational behind that shield. As this heatshield also acts as a shielding for particle radiation (up to certain energies) this creates a very specific environment for studying the effects of the remaining high-energy radiation on the imaging instruments aboard Solar Orbiter. At the same time, the obtained high-resolution imaging observations can help to identify and characterize the solar source regions associated with SEP events.

⋆ Corresponding author: `krzysztof.barczynski@pmodwrc.ch`
⋆⋆ Formerly at PMOD and ETH Zurich, Switzerland

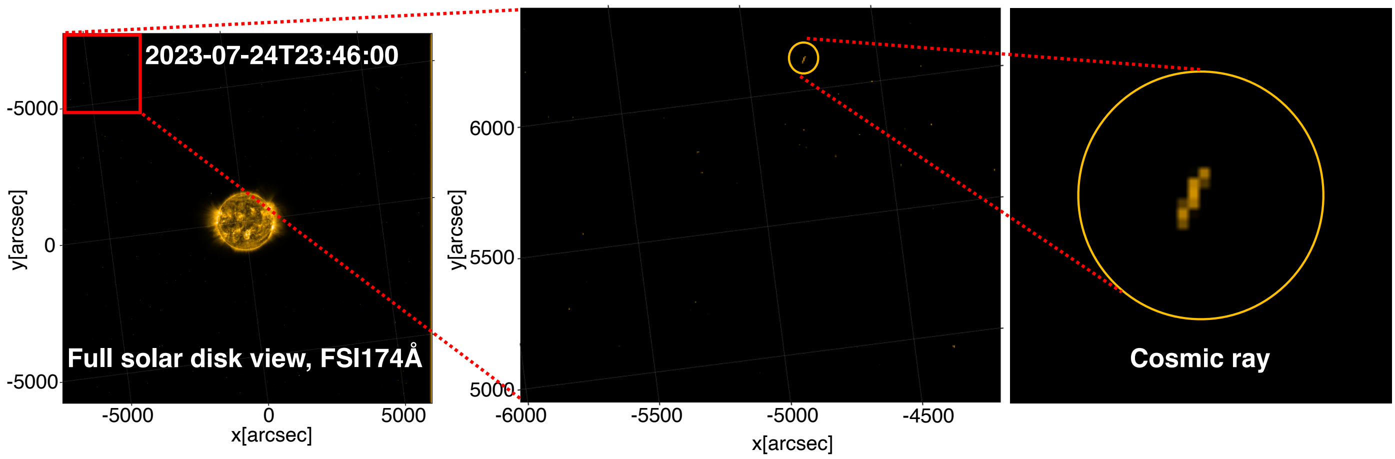

Fig. 1: Detection of a cosmic ray during full-disk solar monitoring with EUI/FSI 174Å. Panel (a) shows the full field of view of EUI/FSI 174Åwith the Sun in the central part of the image. It also contains a small region outside the solar disk which is highlighted in red colour box, which is zoomed in panel (b). The yellow circle indicates the position of one of the detected cosmic rays, which is zoomed and presented in details, in panel (c).

Energetic particle hits (abbreviated hereafter as EPHs) are observed as a strong but short-duration localized increase of the signal in EUV images. Figure 1 shows an example of such a particle hit in an observation of the Extreme Ultraviolet Imager (EUI) onboard the Solar Orbiter spacecraft. While the left panel shows the whole image taken with the EUI Full Sun Imager (FS1, 174 Å filter), the strong zoom in the right two panels reveals the appearance of a signal streak over several pixels that corresponds to an energetic particle hit.

The aim of this paper is to report on the solar energetic particle hits (SEPHs) that have been observed in the EUI-FSI instrument during the Solar Orbiter mission from the beginning of the nominal mission phase (i.e. the systematic switch-on of remote-sensing instruments) in November 2022 up to the latest processed observations in March 2026. We detail 1) how these solar energetic particles can be detected in the image data with an adapted algorithm for cosmic ray detection, 2) how their energy can be characterized by comparison with the signal of the Energetic Particle Detector onboard Solar Orbiter, and 3) how these events are distributed in relative strength and time over the mission duration that includes the activity maximum of the current solar cycle 25. To this end, we first describe the instruments used in our analysis (Section 2), explain then the detection methodology (Section 3), before presenting an example event of solar energetic particle hits (in Section 4). We then present in Section 5 the first catalog of high-energy SEP events that have been identified in the EUI-FSI images. The results are then discussed in Section 6, and the main conclusions are presented in Section 7.

2. Instruments description

Solar Orbiter is an ESA-led mission developed in collaboration with NASA. The mission was launched in February 2020 to observe the Sun from an elliptical solar orbit, periodically reaching distances to the Sun as close as 0.29 AU. Solar Orbiter carries ten scientific instruments. Six instruments provide remote-sensing observations, while four instruments perform in situ measurements of the space environment in the vicinity of the spacecraft. In our analysis, we focus on two instruments: the Extreme Ultraviolet Imager (EUI) and the Energetic Particle Detector (EPD).

2.1. Extreme Ultraviolet Imager (EUI)

The Extreme Ultraviolet Imager (EUI) observes the solar disk using three telescopes. The Full Sun Imager (FSI) is a full-disk telescope equipped with two filters centered at 304 Å and 174 Å, covering the solar chromosphere and corona, respectively. The two High Resolution Imagers (HRI) observe the Sun in the Lyman-α passband centered at 1216 Å (HRI-Ly) and in the 174 Å passband (HRI-EUV). These instruments provide information on chromospheric hydrogen Lyman-α emission and coronal emission from plasma at temperatures of approximately 1 MK, respectively.

For the analysis of solar energetic particle hits, we use images from the Full Sun Imager in both channels. The EUV photons are detected by CMOS active pixel sensor (APS) detectors with a size of 3072×3072 pixels for the full-disk detector and an individual pixel size of 10 µm. The measured signal is proportional to the solar photon flux received within the pixel's narrow field of view and the corresponding passband. Then, the received photons are converted to electric signal, which is subsequently converted into digital numbers. In this study, we use Level-1 (L1) data obtained from the EUI team database at the Royal Observatory of Belgium: `https://www.sidc.be/EUI/data/L1/`. The same data is also publicly available in the Solar Orbiter archive within the ESA HelioPhysics Archive (HPA): `https://hpa.esa.int`.

2.2. Energetic Particle Detector (EPD)

The Energetic Particle Detector (EPD) onboard Solar Orbiter provides in-situ measurements of charged particles above the energy range of the quasi-continuous solar wind. This allows for a systematic study of solar energetic particles (SEPs) that are emitted from highly variable solar and heliospheric sources - including solar flares, CMEs, and stream interaction regions (SIRs). As described in detail in **?**, the EPD instrument measures electrons up to a few tens of MeV, as well as protons and heavy ions up to a few hundred Mev/nuc. To cover this wide range of particles and energies, the instrument consists of four sensors: the Suprathermal Electrons and Protons (STEP), the Suprathermal

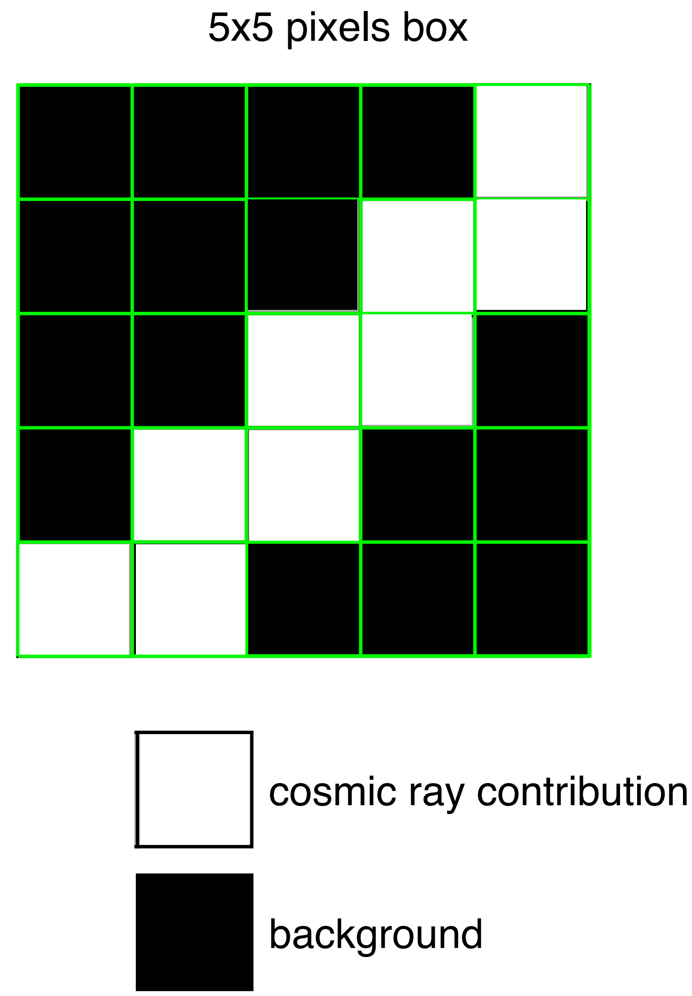

Fig. 2: Example of a (5×5)-pixel box centered on the tested pixels. The white pixels represent pixels affected by cosmic rays, while the black pixels represent the background. We assume that a single cosmic-ray event can affect a maximum of nine pixels in the box.

Ion Spectrograph (SIS), the Electron Proton Telescope (EPT), and the High Energy Telescope (HET).

For this study on high-energy particle hits in EUI, we are focusing mainly on HET measurements for comparison with the EUI signal. The HET sensor consists of four telescopes with fields-of-view (FOVs) in the sun, anti-sun, north, and south direction. For each of these four telescopes, the geometry factor is 0.27 $\mathrm{cm^2 sr}$, which can be further reduced to 0.01 $\mathrm{cm^2 sr}$ when strong particle events occur so that these can be measured without pile-up effects in the sensor electronics. We also note that the ion signal of HET naturally contains a component of Anomalous Cosmic Rays (ACR) that is typically most pronounced in the low to mid MeV/nuc range, and Galactic Cosmic Rays (GCR) that start to become significant at the very high energy end of the measurement range at a few hundred MeV/nuc. However, these ion components provide a relatively constant background that do not play a significant role when strong solar energetic particle events are present that reach up to these energies.

3. Methodology

Our aim is to provide an automatic method for the detection of solar energetic particles and to provide statistics about the number of solar energetic particle hits in the EUI images. To detect such energetic particle hits, we use a method that was originally developed by **Hochedez and Gissot** for SOHO/EIT observations of the full Sun. In a similar way we restrict our method here to EUI-FSI images as these allow the detection of bright signals in wide dark areas of the image away from the solar disk - where clearly no solar photon signal is expected. This area outside the solar disk is critical to our study because this part of the solar image usually does not contain solar structures but is dominated mostly by noise. Here, the assumption can be well-justified that pixels affected by energetic particles show a substantially stronger signal than the surrounding pixels. Naturally, energetic particle hits also affect the HRI detectors. However, their detection can be more difficult due to the high intensity and strong dynamics of the solar structures. The detection of solar energetic particles in HRI images is therefore beyond the scope of this paper. We finally note that an individual high energy particle can have solar origin or be part of the ubiquitous background of cosmic rays (e.g. ACR or GCR). Yet, this cosmic background shows relatively little temporal variability, and at the time of strong solar particle events its contribution is typically exceeded by solar energetic particles up to certain energies in the mid to high MeV range. With the algorithm described in the following, we are able to detect time periods where we find large amounts of energetic particle hits within the same image (or a series of successive images), which then allows us to categorize these time periods as related to solar particle events.

3.1. Algorithm

To identify solar energetic particle signatures, we first check whether a pixel shows a significantly higher intensity than its surrounding local background. We define the local neighborhood as a region of 5×5, thereafter called 5×5 block. This region contains 25 pixels and, compared with the full size of the CMOS detector, it is sufficiently small that we assume that it represents the local background around the pixel of interest. We also tested a smaller blocks, such as 3×3 pixels, but it provides very limited information about the spatial structure of the signal and is therefore considered too small to yield reliable statistics. Going to larger blocks would on the other hand limit the statistics of the particle hits that can be detected in one image. Therefore, we decided to use a block of 5×5 pixels.

The next step is to estimate the background intensity. Some of the pixels within the 5×5 blocks may belong to the actual bright feature and does not represent the background. Therefore, we sort the pixels according to their intensity and exclude the nine brightest pixels. We select nine pixels because solar energetic particles can affect up to nine pixels arranged along the diagonal (see Figure 2). The remaining 16 darkest pixels are used to represent the local background. These pixels are used to calculate the mean local background intensity and its standard deviation, which characterizes the variation of the background intensities around the mean value. The mean intensity and standard deviation are calculated independently for each 5×5 blocks. Finally, the algorithm calculates the standardized intensity excess, S, for cosmic-ray identification, which we defined as:

$$S = \frac{I_{\mathrm{max}} - \mu_{\mathrm{bck}}}{\sigma_{\mathrm{bck}}}. \quad (1)$$

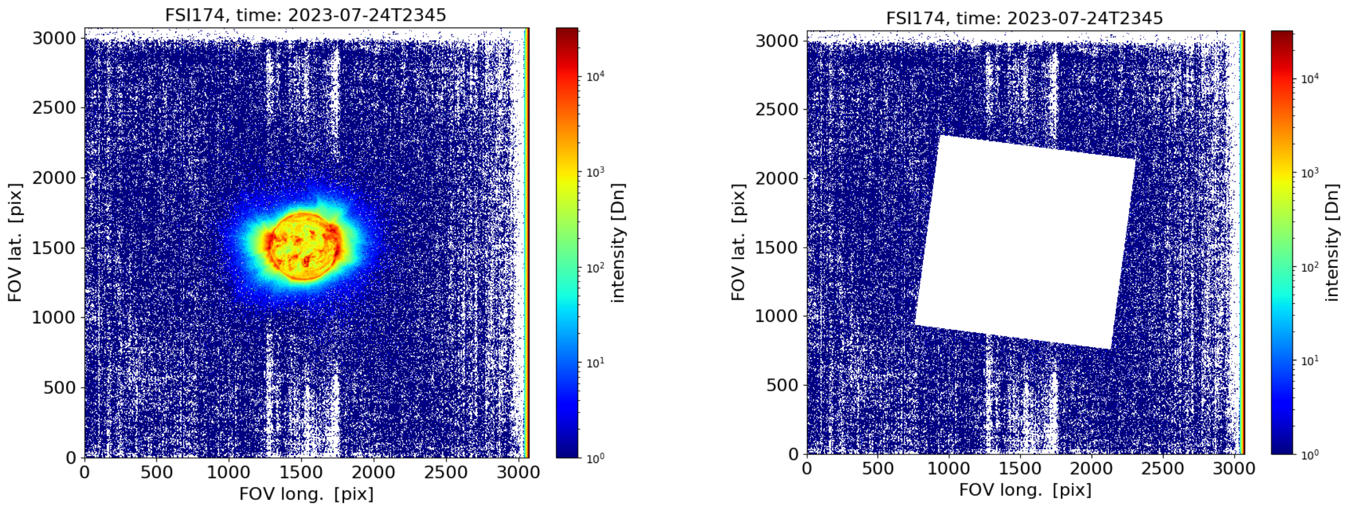

Fig. 3: Exclusion of the full solar disk. (a) Image shows the full field of view with the full solar disk and (b) corresponding image after exclusion of the solar disk.

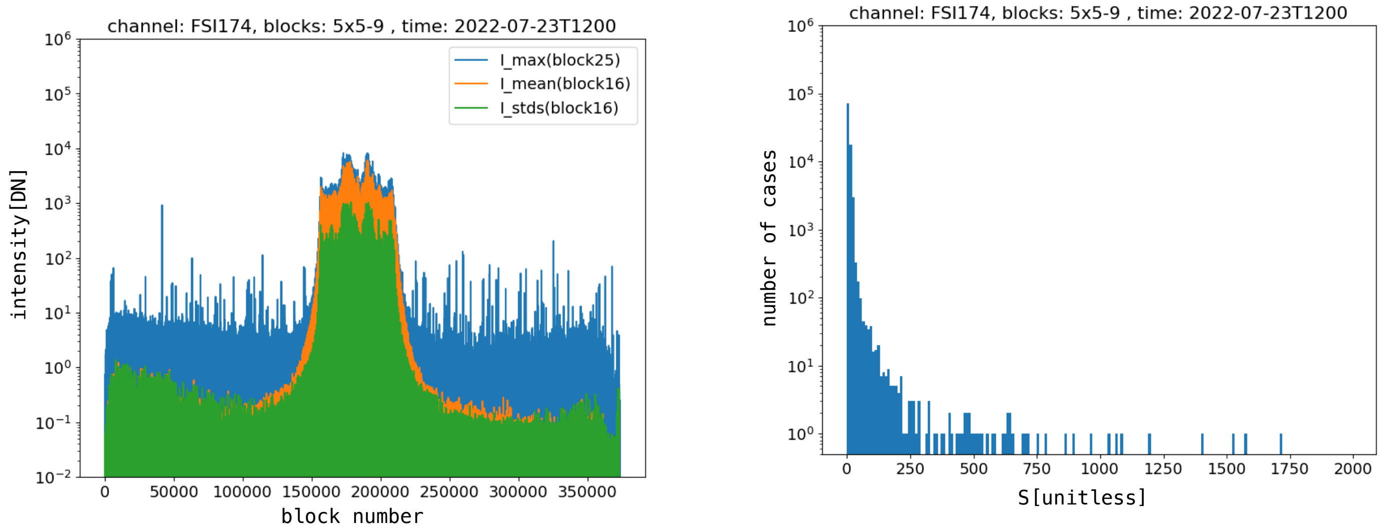

Fig. 4: Statistical intensity properties obtained from individual image blocks. The left panel shows the maximum intensity, mean background intensity, and standard deviation of the background intensity for each block. The right panel shows the distribution of increasing standardized intensity excess.

, where the mean local backround intensity is defined as

$$\mu_{\text{bck}} = \frac{1}{16} \sum_{i=1}^{16} I_i. \tag{2}$$

and the standard deviation of the local background intensity is defined as:

$$\sigma_{\text{bck}} = \sqrt{\frac{1}{16} \sum_{i=1}^{16} (I_i - \mu_{\text{bck}})^2}. \tag{3}$$

.

Our algorithm divides the full-disk image into non-overlapping 5×5 pixel blocks. The first block starting at the beginning of the image array. If the image dimensions are not divided by five, the pixels at the edges of the detector full field of view are removed before defining the block positions. Thus, up to four pixels in both the row and column directions may be excluded. For the typical FSI images used in our analysis, two pixels are removed in both the x and y directions, corresponding to approximately 0.13% of the total image area.

The FSI images contain the full solar disk, which is usually located close to the centre of the image. However, its position can vary depending on the spacecraft pointing configuration. By default, the solar disk is not masked, but the algorithm provides the option to apply a mask when required. If the mask is activated, the algorithm excludes a rectangular region around the Sun such as in Figure 3. The dimension of the mask being defined as a multiple of the solar radius, where the default masking has a size of three solar radii.

3.2. Detection

The algorithm provides the standardized intensity excess; however, to detect solar energetic particle signatures, it is necessary to define a detection threshold. The data obtained from the

EPD provide a reference information about SEP events. Based on the EPD observations, we selected days with and without SEP events (Figure 5). By comparing the observations obtained during SEP events with observation from periods without SEP events, we empirically determined a threshold of 500 for SEP detection:

$$\frac{I_{\text{max}} - \bar{I}_{\text{background}}}{\sigma_{\text{background}}} > 500 \tag{4}$$

The algorithm counts the number of individual blocks in which solar energetic particle signatures are detected. The detection threshold was chosen as a compromise between reliable particle detection and reducing false-positive detections related to instrumental effects, such as electronic noise and hot pixels.

3.3. SEPs in a time function

SEP events produce different numbers of SEPs. Moreover, the number of detected SEPs changes with time during an event. To study the temporal distribution of SEP detections, we added a procedure to the algorithm that allows it to read multiple FITS files containing FSI images, calculate the number of SEP detections in each image, and finally create a plot showing the number of detected SEPs as a function of time.

4. SEP Hits during the event on 23 July 2024

To present an example of such temporal evolution, we selected the SEP event observed by EPD between 23 and 25 July 2023. The STEP+EPT+HET observations show an increase in the energy of the detected ions up to approximately 100 MeV (Figure A.1(a)). At the same time, STEP+EPT detected a significant increase in electrons originating from the Sun (Figure A.1(b)), together with a clear increase in the differential intensity of ions in six selected energy channels (Figure A.1(c)).

Particles associated with this SEP event also reached the EUI detector, producing a clear and relatively sharp increase in the number of detected solar energetic particles (Figure A.1(d)), from a background level of approximately 10 SEPs per image to a maximum of around 300 SEPs per image.

5. Catalogue

SEPs are observed throughout the entire solar cycle; therefore, their monitoring should be performed continuously. To identify SEP events that are sufficiently intense to affect the EUI detector, we create a catalog of SEP events associated with ion detections above 10 MeV. We selected this threshold, because for events below this threshold we never identified SEPs in EUI/FSI. For events with ion energies above 10 MeV, we defined the time intervals based on the EPD ion flux plots. We then applied our SEP detection algorithm to the EUI/FSI observations within these time intervals. The algorithm determine the number of SEP events detected by the EUI/FSI instrument and generate a plot with their temporal distribution.

We analyzed observations from two FSI channels acquired between 2020 and August 2026. Based on this analysis, we created a catalog of SEP events that affected the EUI/FSI observations. The primary aim of the catalog is to characterize which SEP events have a measurable impact on the CMOS camera onboard Solar Orbiter. This catalog provides a systematic overview of the occurrence and temporal distribution of SEP events affecting the EUI/FSI detector and can be used to support the continuous monitoring of SEP-induced effects throughout the solar cycle.

The catalogue contains 27 events recorded between 2022 and 2026. In 2022, four events were identified (20 January, 21 March, 30 August, and 6 September); in 2023, seven events occurred (22 May, 25 July, 6, 8, and 11 September, 10 October, and 14 November); and 2024 had the highest number, with eleven events (11 February, 23 March, 20 May, 23 and 27 July, 5 and 9 September, 9 and 27 October, 21 November, and 8 December). In 2025, two events were recorded (21 August and 11 November), while 2026 contained three events (19 January, 10 May, and 5 June).

6. Discussion

One of the advantages of the EUI detector is its ability to measure the spatial distribution of SEPs. In contrast, most conventional particle detectors provide only integrated particle count rates, without information on the spatial distribution of individual events. For the EUI detector, each (5×5) pixel block can be considered as an individual effective pixel with a physical size of (50×50 μm). The detector contains (614×614) such blocks, corresponding to a total physical area of approximately (30.72×30.72 mm). Therefore, the smallest spatial scale that can be resolved in our analysis is (50 μm).

In addition to the remote-sensing observations, Solar Orbiter provides synoptic observations with the EUI/FSI instrument. These observations are acquired almost continuously, with a typical temporal cadence of 10–15 minutes. This observations provides almost continous information about the stong SEPs event, and also information about the dynamics and evolution of the solar structures based on FSI imaging data. Therefore, EUI/FSI can help with identification of the source region of the SEP event, and measure also impact on the same event for a detector.

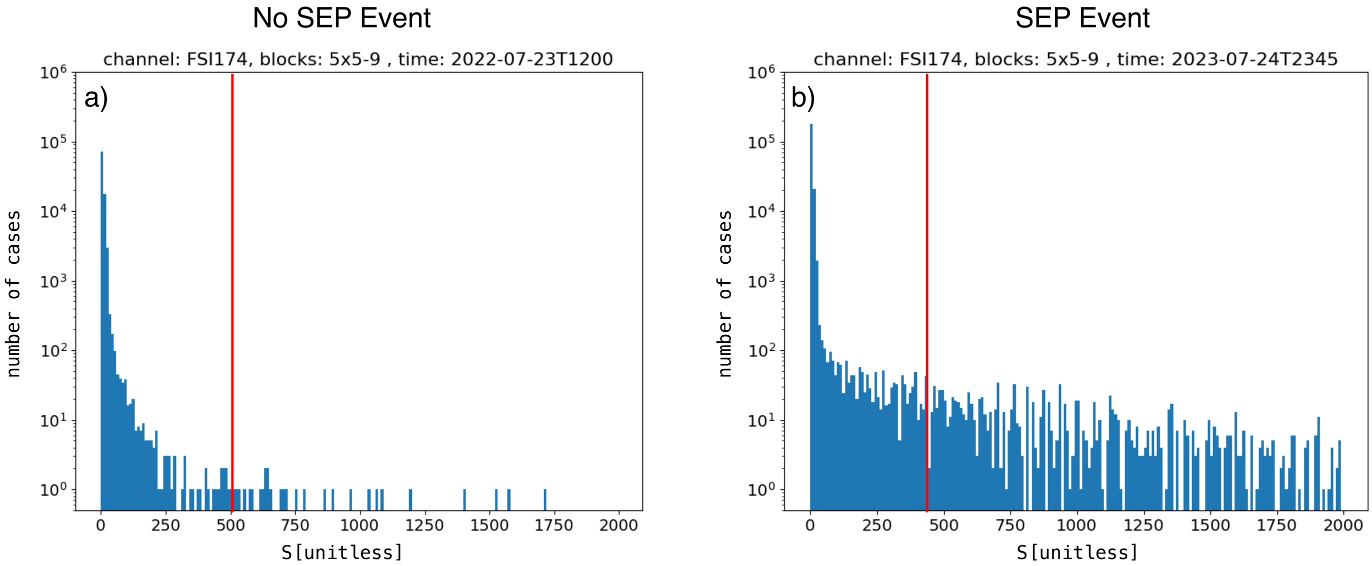

Fig. 5: Distribution of the increasing standardized intensity excess for (a) situation without SEPs and (b) SEP events. The red line indicates the cosmic-ray detection threshold.

7. Conclusions

EUI/FSI can detect the effects of high-energy SEPs on its CMOS detector. The analysis indicates sensitivity to SEP events involving ions with energies above approximately 10 MeV.

References

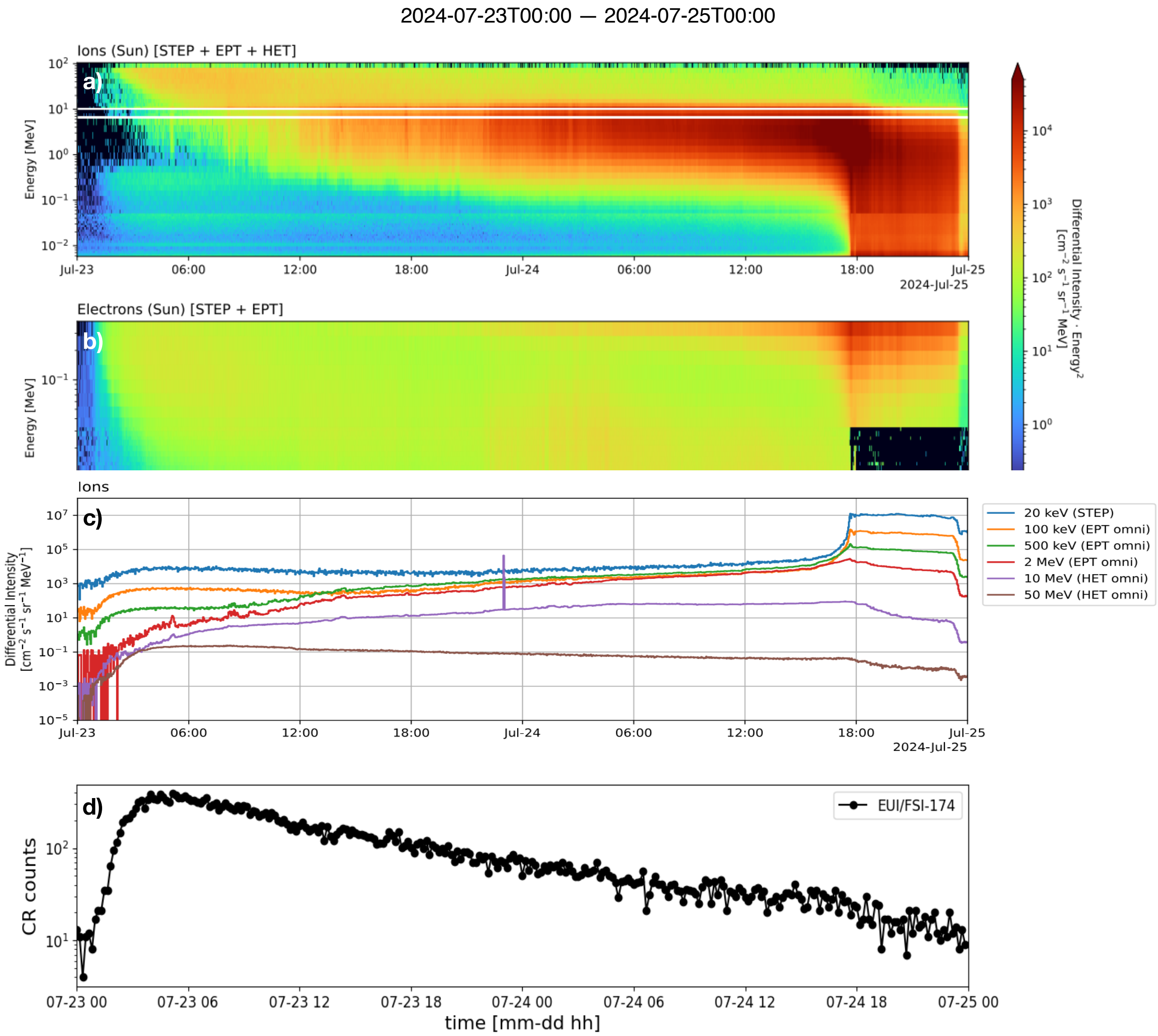

Fig. 6: The solar energetic particle event observed by EPD and EUI. The ions (a) and electrons (b) related to the solar energetic particle event were detected by EPD. The plots show the measured particle energies over a two-day interval. Panel (c) presents the differential intensity analysis for six selected wavelengths. Panel (d) shows the detection of cosmic rays obtained from EUI observations.

Appendix A: Appendix section

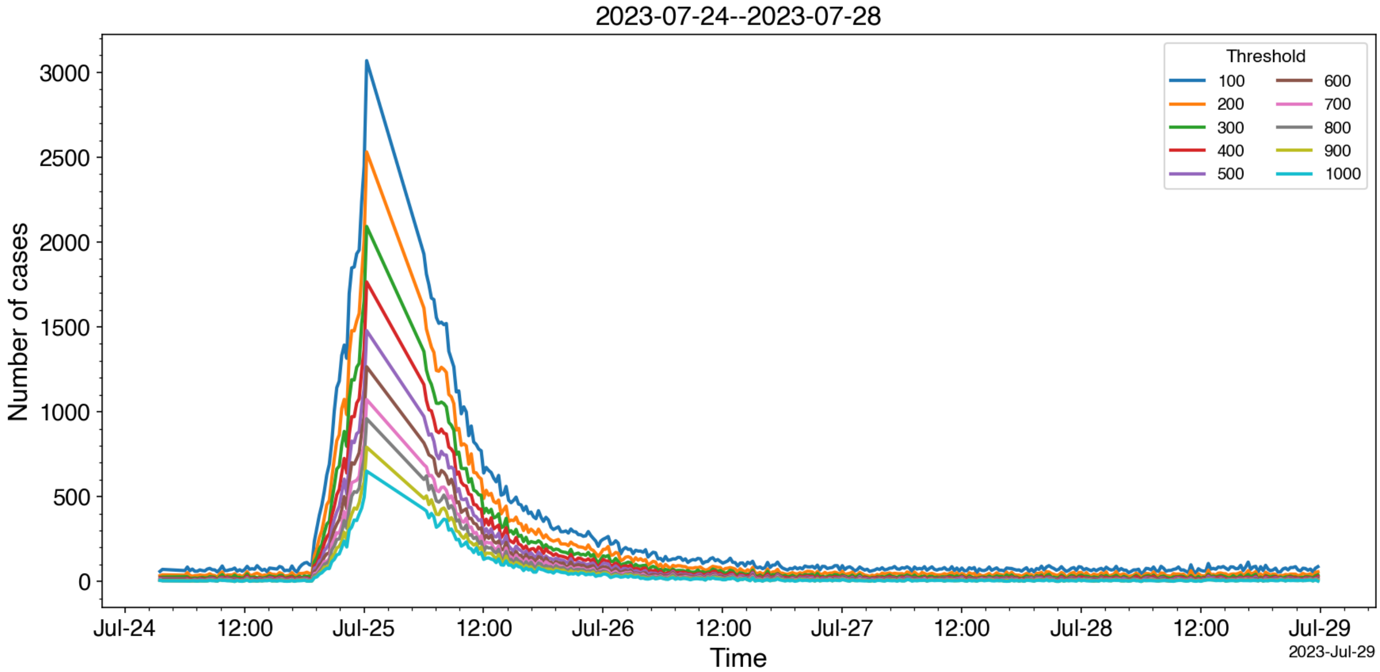

Fig. A.1: Test of the detection threshold for Solar Energetic Particle (SEP) events.